

Ptychographic Imaging of Magnetic Domain Wall Dynamics

Tim A. Butcher,^{1,2,*} Nicholas W. Phillips,^{1,3} Abraham L. Levitan,¹ Jörg Raabe,¹ and Simone Finizio¹

¹*Paul Scherrer Institut, 5232 Villigen PSI, Switzerland*

²*Max Born Institute for Nonlinear Optics and Short Pulse Spectroscopy, 12489 Berlin, Germany*

³*Minerals Resources CSIRO, 3168 Clayton, Australia*

(Dated: August 27, 2024)

The dynamics of domain walls in a square of permalloy ($\text{Ni}_{81}\text{Fe}_{19}$; Py) upon excitation with an oscillating magnetic field of 4 mT amplitude were recorded by pump-probe ptychography with X-ray magnetic circular dichroism (XMCD) at the Ni L_3 -edge. The 2.5 μm Py square of 160 nm thickness forms a vortex flux-closure pattern with domain walls that fall into alternating out-of-plane magnetization states due to the interplay of in-plane shape and growth-induced perpendicular anisotropies. Dynamic modes of the domain wall structure were excitable along with the vortex core gyration with frequencies of 500 MHz and 1 GHz. Micromagnetic simulations served to corroborate the imaged domain wall motion.

Magnetization dynamics lie at the heart of the technological applications of magnetic materials. Of particular interest are the excitations of magnetic micro- and nanostructures that feature Landau flux-closure magnetization patterns in order to minimize their stray field [1]. In the case of micron-sized magnetic squares, the flux-closure pattern consists of four triangular domains with the magnetization in-plane (IP) and arranged head-to-tail. The domains are separated by domain walls at which the magnetization directions change by 90°. At the center of the square lies a vortex core in which the magnetization points into or out of the plane. Vortices contain two degrees of freedom: the chirality given by the rotation direction of the IP magnetization direction and the out-of-plane (OOP) orientation of the vortex core. The combination of these are of relevance for applications in data storage [2]. The vortex core motion under excitation can also excite spin waves that are central to the field of magnonics [3, 4]. However, the domain walls themselves are also excited by time-dependent magnetic fields and can develop their own dynamics. Here we report the observation of a non-trivial domain wall structure in a micron-sized square of 160 nm thick permalloy ($\text{Ni}_{81}\text{Fe}_{19}$; Py) and its excitation by an oscillating magnetic field with pump-probe ptychographic imaging.

Microscopic techniques employing synchrotron radiation have been highly successful in tracking magnetization changes by providing sequences of time-resolved images obtained with X-ray magnetic circular dichroism (XMCD) at the X-ray absorption edges of magnetic elements [3–9]. The XMCD contrast is maximized in the soft X-ray energy range, which includes the L-edges of the magnetic transition metals. Scanning transmission X-ray microscopy (STXM) in which the sample is scanned through the X-rays in the focal point of a zone plate has established itself as one of the most popular methods for imaging magnetic dynamics [3, 10, 11]. The transmitted intensities are measured by a point detector with

a larger bandwidth than the repetition rate of the synchrotron source (500 MHz for the Swiss Light Source). This is typically achieved by using a small area avalanche photodiode and allows the time-resolved imaging of magnetization dynamics at numerous excitation frequencies [12]. Nonetheless, despite the achievable temporal resolution, which can be pushed beyond the limit imposed by the duration of the X-ray pulses [13], the shortcoming of STXM lies in the spatial resolution. This is dictated by the zone plate and is around 25 nm for regular measurements. The coherent diffractive imaging method of soft X-ray ptychography [14] is capable of achieving a spatial resolution that surpasses that of STXM and has been successfully employed for magnetic imaging [15, 16]. The setup can be seen in Fig. 1(a). Circularly polarized soft X-rays are focused by a zone plate and illuminate the sample downstream of the focal plane. An order selecting aperture (OSA) serves to remove higher orders of X-rays diffracted by the zone plate. The X-rays are scattered by the sample and registered with a 2D pixelated detector. Complex-valued images are reconstructed from the diffraction patterns of overlapping points of the sample that are obtained by scanning it through the beam. Compatible pixelated detectors do not have the necessary bandwidth to resolve individual X-ray bunches and therefore ptychography currently only enables the imaging of dynamics in pump-probe mode with the excitation frequencies locked to an integer multiple of the repetition rate of the synchrotron pulses [17].

The analyzed sample was a Py square with 160 nm thickness and 2.5 μm diameter on an X-ray transparent Si_3N_4 membrane (see Methods section). Ptychographic imaging was performed at the Ni L_3 -edge (856 eV) and XMCD maps of the OOP magnetization M_z were obtained with circularly polarized X-rays at normal incidence on the sample. The ptychographic XMCD image of the static Py square is shown in Fig. 1(b), together with the expected normal component of the magnetization simulated using the MuMax³ finite-difference framework [18]. The XMCD images were calculated as the difference of the amplitudes of the ptychographic reconstructions for left- and right-hand circularly polarized

* tim.butcher@psi.ch

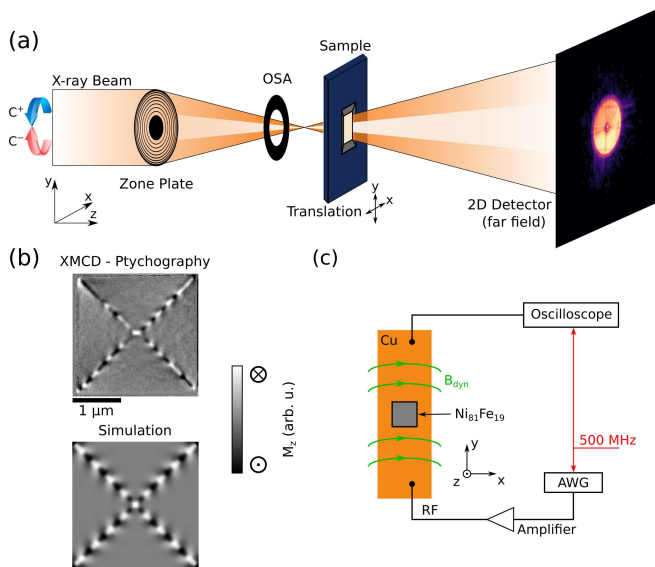


FIG. 1. (a) Soft X-ray ptychography in defocused probe mode. Diffraction patterns from overlapping regions on the sample are captured. (b) XMCD amplitude image of the static Py square at the Ni L_3 -edge and the simulated M_z distribution. Subtraction of the images with opposing X-ray helicities results in the XMCD image. (c) Sketch of the setup for the excitation in pump-probe mode. An RF current from an arbitrary waveform generator (AWG) causes a periodic Oersted field in x-direction, which is frequency locked to the 500 MHz bunches of the synchrotron.

illumination. A Landau flux closure pattern is formed in the Py square and the IP domains show no XMCD contrast in this geometry. The components that have an OOP component are the vortex core and the domain walls that separate the triangular domains.

Inspection of the vortex core in the XMCD image shows that it is horizontally elongated with a width of 120 nm and 50 nm height. The likely explanation for this is a slight uniaxial IP anisotropy arising during the growth of the sample [19]. Furthermore, the XMCD contrast of the vortex core is not sharp, which evinces a barrel-like magnetic vortex with columnar structure [9]. Such a 3D modification in which the diameter of the vortex core diameter is minimized at the surfaces is often observed in thick magnetic microstructures.

The thickness of the Py square also affects the configuration of the approximately 80 nm wide domain walls, which were found to have split into different regions of inward and outward magnetization. This is opposed to the common case in which the magnetic moments undergo an out-of-plane rotation in unison akin to a Bloch wall during the 90° reorientation. The explanation lies in the fact that the 160 nm thick Py film has a weak perpendicular anisotropy and is on the verge of flipping the magnetization to an OOP orientation with stripe domains [20–22]. The perpendicular anisotropy originates in the shape anisotropy stemming from the columnar growth of the Py thin film. Although the growth-induced anisotropy is

weak, it is sufficient to force the domain wall into regions of alternating magnetization directions so that it appears as a striped pattern in the XMCD image.

The simulated ground state of the Landau flux-closure pattern can adopt such a configuration by tuning the perpendicular magnetic anisotropy, which imparts stripes of uniform period to the domain wall. Although the experimentally observed aperiodic domain wall configuration differs from the ideal theoretical case due to the presence of pinning sites and local variations of the anisotropy, two other experimental observations can be verified in the simulations. Firstly, the arrow shape of the stripes with a faintly protruding OOP magnetization of the shafts into the domains. Secondly, the abrupt switching of the magnetization direction at the corners of the square in order to minimize the stray field.

Subsequently, the dynamics of this flux closure state were investigated. For this, the sample was excited by the radio-frequency (RF) Oersted field from a Cu stripline fabricated on top of the Py square, which is sketched in Fig. 1(c). Frequency locking of the RF current to harmonics of the probing signal at 500 MHz enabled pump-probe imaging of the dynamics by ptychography with XMCD. Varying the delay of the magnetic excitation with respect to the X-ray pulses allows dynamic imaging with temporal resolutions limited to the X-ray bunch length (70 ps FWHM at the Swiss Light Source). The results for RFs of 500 MHz and 1 GHz are displayed in Figs. 2(a,b), respectively. The corresponding animations can be viewed in the supporting information.

The gyration of the vortex core is not only accompanied by bending of the domain walls, but also by excitation modes within them. At 500 MHz, stretching and contraction of several sections of the domain walls by approximately 200 nm are observed as the domain walls slightly bend during the cycle. This is particularly evident in the bottom right part of the domain walls in which one segment almost completely merges with its neighbor during the periodic motion around one node. The behavior is also observed at 1 GHz, but the reaction of the domain walls is more rigid. Above excitations of 1 GHz and up to the maximum probed frequency of 3 GHz, the domain walls are unable to follow and the system remains unperturbed. No excitation of spin-waves was observed in the domains at these frequencies. Although the ground state of the domain wall displayed in Fig. 1(b) is reminiscent of the one-dimensional propagation of spin waves in domain walls [8, 23], no frequency or wave vector can be assigned to the domain wall excitation detected here.

The detected domain wall modes were reproduced in micromagnetic simulations of the dynamics at 500 MHz, which are shown in Fig. 3 (animations in the supporting information). The translation of the domain wall and pumping of its segments are strongly dependent on the magnitude of the perpendicular magnetic anisotropy. Faint spin waves can be seen to emanate from the arrow shaped segments of the domain walls in the simulation,

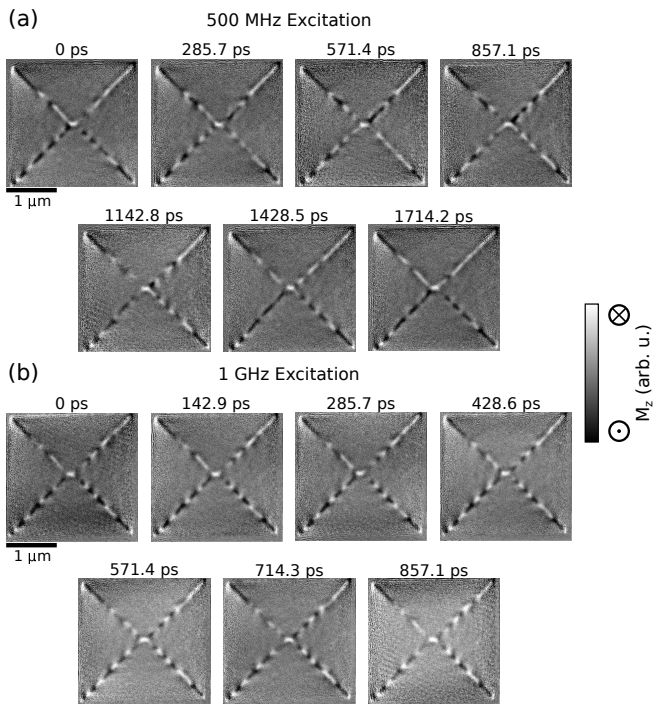


FIG. 2. XMCD image sequences of the magnetization configuration upon excitation of the Py square with a 4 mT amplitude in the horizontal direction (animations in the supporting information). Gyration of the vortex core, motion of the domain walls and their segments are observed. (a) 500 MHz excitation. (b) 1 GHz excitation.

but these are not detectable in the XMCD images in Fig. 2(a), as their contrast is low and they are likely insufficiently reproducible to appear in a pump-probe measurement in addition.

For the purpose of understanding the magnetization changes within the Py square during a 500 MHz excitation, the cross section of the simulated magnetization distributions for a cut along the domain wall are summarized in Fig. 3(b). The simulations feature the accordion-like motion of the domain wall segments during the excitation period in which the up and down regions are alternately compressed. Notably, the magnetization points IP at the surface above and below the domain wall segments in opposite directions. These structures are known as Néel caps that are encountered around Bloch domain walls and serve to minimize the magnetostatic energy at the surface [24, 25]. In two dimensions, the combination of the Bloch walls and Néel caps resemble vortices that curl around the different sections of the domain wall. The Néel caps move in unison with the 90° Bloch-like domain wall segments in the studied Landau flux closure pattern.

In conclusion, the magnetic domain wall configuration of a flux-closure system with a thickness on the brink of a change to OOP magnetization was studied by ptychographic imaging. This onset of growth-induced perpendicular magnetic anisotropy divides the 90° Bloch-like domain walls into several segments of alternating magne-

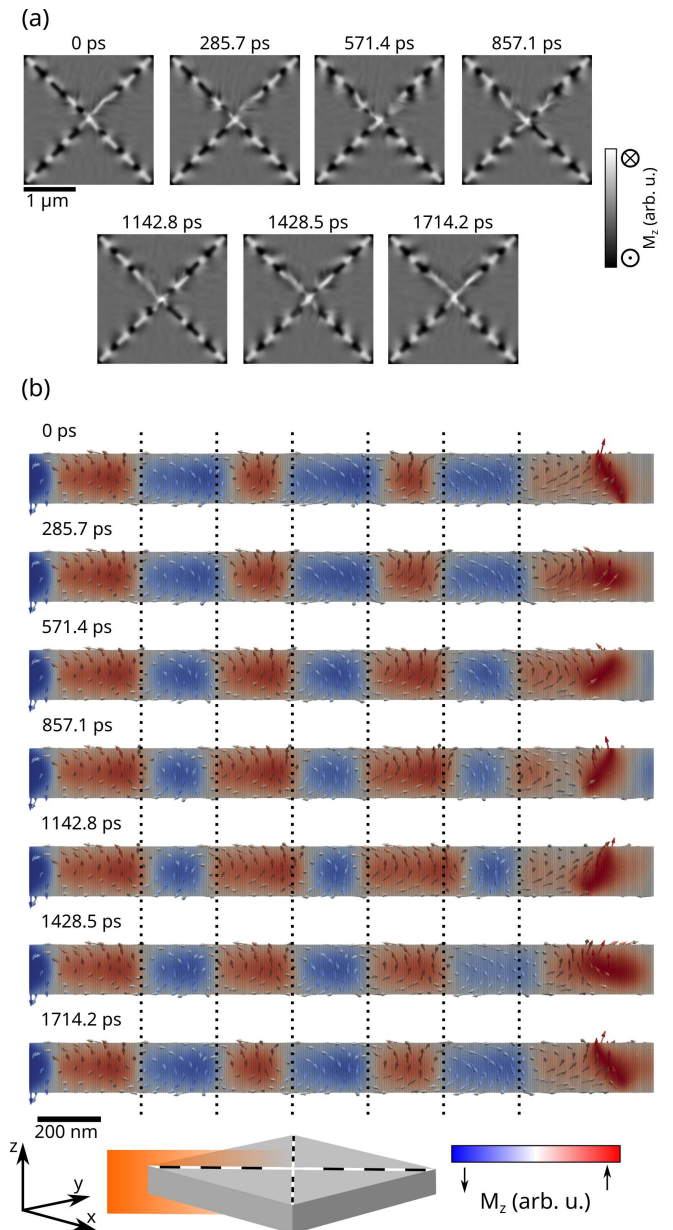


FIG. 3. Micromagnetic simulations of the magnetization dynamics with a 500 MHz excitation. (a) The OOP component M_z in the domain walls follows the experimental observation in Fig 2(a) (animations in the supporting information). (b) 2D configuration of \mathbf{M} in the plane along the domain wall up to the vortex core during 500 MHz excitation. The geometry of the cross section is illustrated below.

tization. A complete switch to OOP magnetization is accompanied by the emergence of stripe domains throughout the Py [20–22] and the observed vortex-like pattern in the domain wall is a precursor of these. The individual components of the domain wall stretch and shrink under RF excitation up to 1 GHz, which was observed experimentally with pump-probe soft X-ray ptychography as well as in micromagnetic simulations. Ptychographic imaging with soft X-rays provides an improvement upon

the spatial resolution of STXM, which will be beneficial for the imaging of magnetic structures with dimensions below 15 nm as well as non-collinear magnetism [16]. Its extension to three-dimensional imaging with laminography, as has already been achieved with hard X-rays [17] and STXM [9], is currently underway. One future development that will revolutionize coherent diffractive imaging will be the extension of event-counting Timepix read-out devices [26] to soft X-ray detectors [27] that will enable the assignment of detection time to incoming photons and dispense with the requirement of frequency locking to the X-ray pulse repetition rate. In the case of imaging magnetic domain wall dynamics, this will permit the study of excitation frequencies lower than 500 MHz at which the emission of one-dimensional spin waves are expected [8].

METHODS

A. Sample Fabrication

A microstructured Py square (2.5 μm wide, 160 nm thick) was patterned on top of a 200 nm thick, $1 \times 1 \text{ mm}^2$ wide Si_3N_4 membrane in the center of a $5 \times 5 \text{ mm}^2$ Si frame (250 μm thick, Silson Ltd.) by electron beam lithography with a Vistec EBPG5000, 100 kV electron beam writer. The lithography was performed by means of lift-off with a bilayer resist composed of a layer of poly(methyl-methacrylate) (4% in Anisole, 3000 rpm for 1 min) spincoated on top of a layer of methyl methacrylate (6% in Ethyl-Lactate, 3000 rpm for 1 min), which was spincoated on top of the Si_3N_4 membrane. A 1 minute soft-bake at 175 $^\circ\text{C}$ was performed for both resists. The resist was exposed with an electron dose of 1550 $\mu\text{C cm}^{-2}$ and developed by immersion in a 1:3 (volume) solution of methyl isobutyl ketone and isopropyl alcohol (IPA), followed by rinsing with pure IPA (each for 45 s). After the deposition of a 160 nm thick Py film from a stoichiometric pellet using a Balzers BAE250 thermal evaporator, where a 10 nm thick Cr seed layer was deposited prior to the Py. The unexposed resist, together with the Py film on top of it was then removed by immersion of the sample in pure acetone followed by rinsing in pure IPA.

A 5 μm wide, 300 nm thick, Cu stripline designed for the generation of a sinusoidal IP magnetic field along the x -axis was fabricated on top of the Py square. This was carried out by electron beam lithography and liftoff with the same recipe.

B. Soft X-ray Ptychography

The Py sample was imaged by soft X-ray ptychography at the Surface/Interface Microscopy (SIM) beamline at the Swiss Light Source. An elliptical Apple II UE56 undulator was used to generate circularly polarized X-rays at the Ni L_3 -edge. The sample-detector distance

amounted to 90 mm and the detector was a 512×512 pixel single photon counting Low Gain Avalanche Diode (LGAD) Eiger with a pixel size of 75 μm . Diffraction patterns were recorded with an exposure time of 200 ms.

The Fresnel zone plate that shaped the beam in order to illuminate the sample with a 1 μm FWHM X-ray beam was Ir zone doubled with 20 nm outer zone width and 500 μm diameter. The zone plate did not have a central stop, so a separate 2 μm thick Au central stop with 100 μm diameter was placed upstream to attenuate the central beam. An order selecting aperture (OSA) was employed to suppress X-rays from higher diffraction orders as in STXM. The Py square was moved through the X-ray beam in a Fermat spiral pattern in steps of 100 nm.

The *Ptychoshelves* software package [28] was used to reconstruct the images with 300 iterations of difference-map [29] followed by up to 500 iterations of maximum-likelihood refinement [30] with orthogonal probe relaxation [31]. The spatial resolution of the image was estimated to be around 10 nm with a Fourier Ring Correlation and the 1-bit criterion. After alignment of the ptychographic reconstructions in order to correct for drifts of the sample, the XMCD images were calculated by subtracting the amplitude images.

C. Excitation setup

Figure 1(c) shows a sketch of the excitation setup. The Py microstructured square was excited by injecting a RF current across the Cu stripline fabricated on top of it, giving rise to an oscillating magnetic field through the Oersted effect. The electrical circuit used for the excitation is schematically depicted in Fig. 1(b). The amplitude of the RF current was selected to generate amplitude of approximately 4 mT. The RF current was generated by a Keysight M8195A arbitrary waveform generator (AWG) with a 64 GSa s^{-1} sampling rate, frequency locked to the 500 MHz master clock of the synchrotron light source, combined with a Minicircuits ZHL-42W+ RF amplifier. The time series was recorded by varying the delay between the master clock and the RF signal generated by the AWG. This was done in a non-sequential pattern in order to avoid misinterpretation of permanent changes to the sample as dynamics [7]. A sequence of 7 phase delays with the pattern [0,5,3,4,1,6,2] were performed. Frequencies of 500 MHz and its harmonics were used up to 3 GHz.

D. Micromagnetic simulations

Static and dynamic micromagnetic simulations were performed by numerically solving the Landau-Lifshitz-Gilbert equation using the finite differences MuMax³ framework [18]. A three-dimensional simulation grid was considered, consisting of a $512 \times 512 \times 16 \text{ px}^3$ lattice with a $4.8 \times 4.8 \times 10 \text{ nm}^3$ cell. The chosen micromagnetic pa-

rameters were saturation magnetization of $M_s = 8 \times 10^5 \text{ A m}^{-1}$, an exchange stiffness of $A_{\text{ex}} = 10^{-11} \text{ J m}^{-1}$, a Gilbert damping constant of $\alpha = 0.01$, and a perpendicular magnetic anisotropy of $K_u = 8.75 \text{ kJ m}^{-3}$. These were determined by matching the simulated static configuration to the XMCD images of the Py microstructured square from ptychography and resulted in an exchange length of about 5 nm. To verify that the size of the discretization was not affecting the results of the micromagnetic simulations, a subset was performed with a $2.4 \times 2.4 \times 2.5 \text{ nm}^3$ discretization. The results of the simulation with the finer grid closely resembled those obtained with the larger grid, but required fewer computational resources and were therefore used. The static configuration, used as the starting point for the time-resolved simulation, was determined by relaxing a symmetric Landau pattern.

For the time-resolved simulation, an oscillating magnetic field with a frequency of either 500 MHz or 1 GHz (in both cases with an amplitude of 4 mT) was applied along the x -axis, which reproduced the experimental configuration. Transient effects caused by the sudden application of the magnetic field were avoided by simulating a 200 ns period prior to the recorded simulated images. The simulated magnetic configuration was then saved at 7 equally distributed instances across one cycle of excitation (either 2 ns for the 500 MHz excitation or 1 ns for

the 1 GHz excitation).

SUPPORTING INFORMATION

Animations of the ptychographic XMCD image sequences in Fig. 2 and the micromagnetic simulations of the magnetization dynamics in Fig. 3(a).

I. ACKNOWLEDGMENTS

Soft X-ray ptychography measurements were performed at the Surface/Interface Microscopy (SIM-X11MA) beamline of the Swiss Light Source (SLS), Paul Scherrer Institut, Villigen PSI, Switzerland. T.A.B. acknowledges funding from the Swiss Nanoscience Institute (SNI) and the European Regional Development Fund (ERDF). N.W.P. and A.L.L. received funding from the European Union's Horizon 2020 research and innovation programme under the Marie Skłodowska-Curie grant agreement no. 884104 (PSI-FELLOW-III-3i). We thank E. Fröjdh, F. Baruffaldi, M. Carulla, J. Zhang, and A. Bergamaschi for the development of the LGAD Eiger detector. The LGAD sensors were fabricated at Fondazione Bruno Kessler (Trento, Italy). We thank M. Langer, S. Mayr, and S. Wintz for the preliminary measurements that preceded this work.

-
- [1] L. Landau and E. Lifshitz, On the theory of the dispersion of magnetic permeability in ferromagnetic bodies, *Phys. Z. Sowjetunion* **8**, 101 (1935).
 - [2] K. Yamada, S. Kasai, Y. Nakatani, K. Kobayashi, H. Kohno, A. Thiaville, and T. Ono, Electrical switching of the vortex core in a magnetic disk, *Nature Mater.* **6**, 270 (2007).
 - [3] S. Wintz, V. Tiberkevich, M. Weigand, J. Raabe, J. Lindner, A. Erbe, A. Slavin, and J. Fassbender, Magnetic vortex cores as tunable spin-wave emitters, *Nat. Nanotechnol.* **11**, 948–953 (2016).
 - [4] S. Mayr, L. Flajšman, S. Finizio, A. Hrabec, M. Weigand, J. Förster, H. Stoll, L. J. Heyderman, M. Urbánek, S. Wintz, and J. Raabe, Spin-wave emission from vortex cores under static magnetic bias fields, *Nano Lett.* **21**, 1584 (2021).
 - [5] J. Raabe, C. Quitmann, C. H. Back, F. Noltling, S. Johnson, and C. Buehler, Quantitative analysis of magnetic excitations in Landau flux-closure structures using synchrotron-radiation microscopy, *Phys. Rev. Lett.* **94**, 217204 (2005).
 - [6] P. Wessels, J. Ewald, M. Wieland, T. Nisius, A. Vogel, J. Viehhaus, G. Meier, T. Wilhein, and M. Drescher, Time-resolved imaging of domain pattern destruction and recovery via nonequilibrium magnetization states, *Phys. Rev. B* **90**, 184417 (2014).
 - [7] F. Büttner, C. Moutafis, M. Schneider, B. Krüger, C. M. Günther, J. Geilhufe, C. Schmising, J. Mohanty, B. Pfau, A. Schaffert, S. Bisig, M. Foerster, T. Schulz, C. Vaz, J. H. Franken, H. J. M. Swagten, M. Kläui, and S. Eisebitt, Electrical switching of the vortex core in a magnetic disk, *Nature Phys.* **11**, 225 (2007).
 - [8] V. Sluka, T. Schneider, R. A. Gallardo, A. Kákay, M. Weigand, T. Warnatz, R. Mattheis, A. Roldán-Molina, P. Landeros, V. Tiberkevich, A. Slavin, G. Schütz, A. Erbe, A. Deac, J. Lindner, J. Raabe, J. Fassbender, and S. Wintz, Emission and propagation of 1D and 2D spin waves with nanoscale wavelengths in anisotropic spin textures, *Nat. Nanotechnol.* **14**, 328–333 (2019).
 - [9] S. Finizio, C. Donnelly, S. Mayr, A. Hrabec, and J. Raabe, Three-dimensional vortex gyration dynamics unraveled by time-resolved soft x-ray laminography with freely selectable excitation frequencies, *Nano Lett.* **22**, 1971 (2022).
 - [10] K. Litzius, I. Lemesch, B. Krüger, P. Bassirian, L. Caretta, K. Richter, F. Büttner, K. Sato, O. A. Tretiakov, J. Förster, R. M. Reeve, M. Weigand, I. Bykova, H. Stoll, G. Schütz, G. S. D. Beach, and M. Kläui, Skyrmion hall effect revealed by direct time-resolved x-ray microscopy, *Nature Phys.* **13**, 170–175 (2016).
 - [11] S. Finizio, K. Zeissler, S. Wintz, S. Mayr, T. Weßels, A. J. Huxtable, G. Burnell, C. H. Marrows, and J. Raabe, Deterministic field-free skyrmion nucleation at a nanoengineered injector device, *Nano Lett.* **19**, 7246 (2019).
 - [12] A. Puzic, T. Korhonen, B. Kalantari, J. Raabe, C. Quitmann, P. Jüllig, L. Bommer, D. Goll, G. Schütz, S. Wintz, T. Strache, M. Körner, D. Markó,

- C. Bunce, and J. Fassbender, Photon counting system for time-resolved experiments in multibunch mode, *Synchrotron Radiation News* **23**, 26 (2010).
- [13] S. Finizio, S. Mayr, and J. Raabe, Time-of-arrival detection for time-resolved scanning transmission X-ray microscopy imaging, *J. Synchrotron Radiat.* **27**, 1320 (2020).
- [14] D. A. Shapiro, Y.-S. Yu, T. Tyliczszak, J. Cabana, R. Celestre, W. Chao, K. Kaznatcheev, A. D. Kilcoyne, F. Maia, S. Marchesini, *et al.*, Chemical composition mapping with nanometre resolution by soft x-ray microscopy, *Nature Photon.* **8**, 765 (2014).
- [15] X. Shi, P. Fischer, V. Neu, D. Elefant, J. C. T. Lee, D. A. Shapiro, M. Farmand, T. Tyliczszak, H.-W. Shiu, S. Marchesini, S. Roy, and S. D. Kevan, Soft x-ray ptychography studies of nanoscale magnetic and structural correlations in thin SmCo_5 films, *Appl. Phys. Lett.* **108**, 094103 (2016).
- [16] T. A. Butcher, N. W. Phillips, C.-C. Chiu, C.-C. Wei, S.-Z. Ho, Y.-C. Chen, E. Fröjdh, F. Baruffaldi, M. Carulla, J. Zhang, A. Bergamaschi, C. A. F. Vaz, A. Kleibert, S. Finizio, J.-C. Yang, S.-W. Huang, and J. Raabe, Ptychographic nanoscale imaging of the magnetoelectric coupling in freestanding BiFeO_3 , *Adv. Mater.* **36**, 2311157 (2024).
- [17] C. Donnelly, S. Finizio, S. Gliga, M. Holler, A. Hrabec, M. Odstrčil, S. Mayr, V. Scagnoli, L. J. Heyderman, M. Guizar-Sicairos, and J. Raabe, Time-resolved imaging of three-dimensional nanoscale magnetization dynamics, *Nat. Nanotechnol.* **15**, 356 (2020).
- [18] A. Vansteenkiste, J. Leliaert, M. Dvornik, M. Helsen, F. Garcia-Sanchez, and B. Van Waeyenberge, The design and verification of MuMax3, *AIP Advances* **4**, 107133 (2014).
- [19] S. E. Stevenson, C. Moutafis, G. Heldt, R. V. Chopdekar, C. Quitmann, L. J. Heyderman, and J. Raabe, Dynamic stabilization of nonequilibrium domain configurations in magnetic squares with high amplitude excitations, *Phys. Rev. B* **87**, 054423 (2013).
- [20] N. Saito, H. Fujiwara, and Y. Sugita, A new type of magnetic domain structure in negative magnetostriction ni-fe films, *J. Phys. Soc. Jpn.* **19**, 1116 (1964).
- [21] T. Iwata, R. J. Prosen, and B. E. Gran, Perpendicular Anisotropy in Polycrystalline Ni-Fe Thin Films, *J. Appl. Phys.* **37**, 1285 (1966).
- [22] S. Finizio, S. Wintz, D. Bracher, E. Kirk, A. S. Semisalova, J. Förster, K. Zeissler, T. Weßels, M. Weigand, K. Lenz, A. Kleibert, and J. Raabe, Thick permalloy films for the imaging of spin texture dynamics in perpendicularly magnetized systems, *Phys. Rev. B* **98**, 104415 (2018).
- [23] K. Wagner, A. Kákay, K. Schultheiss, A. Henschke, T. Sebastian, and H. Schultheiss, Magnetic domain walls as reconfigurable spin-wave nanochannels, *Nat. Nanotechnol.* **11**, 432–436 (2016).
- [24] S. Foss, R. Proksch, E. D. Dahlberg, B. Moskowitz, and B. Walsh, Localized micromagnetic perturbation of domain walls in magnetite using a magnetic force microscope, *Appl. Phys. Lett.* **69**, 3426 (1996).
- [25] F. Cheynis, A. Masseur, O. Fruchart, N. Rougemaille, J. C. Toussaint, R. Belkhou, P. Bayle-Guillemaud, and A. Marty, Controlled switching of Néel caps in flux-closure magnetic dots, *Phys. Rev. Lett.* **102**, 107201 (2009).
- [26] A. Tremsin and J. Vallergera, Unique capabilities and applications of Microchannel Plate (MCP) detectors with Medipix/Timepix readout, *Radiat. Meas.* **130**, 106228 (2020).
- [27] A. S. Tremsin, J. V. Vallergera, O. H. W. Siegmund, J. Woods, L. E. De Long, J. T. Hastings, R. J. Koch, S. A. Morley, Y.-D. Chuang, and S. Roy, Photon-counting MCP/Timepix detectors for soft X-ray imaging and spectroscopic applications, *J. Synchrotron Rad.* **28**, 1069 (2021).
- [28] K. Wakonig, H.-C. Stadler, M. Odstrčil, E. H. R. Tsai, A. Diaz, M. Holler, I. Usov, J. Raabe, A. Menzel, and M. Guizar-Sicairos, *PtychoShelves*, a versatile high-level framework for high-performance analysis of ptychographic data, *J. Appl. Cryst.* **53**, 574 (2020).
- [29] P. Thibault, M. Dierolf, A. Menzel, O. Bunk, C. David, and F. Pfeiffer, High-resolution scanning x-ray diffraction microscopy, *Science* **321**, 379 (2008).
- [30] M. Odstrčil, A. Menzel, and M. Guizar-Sicairos, Iterative least-squares solver for generalized maximum-likelihood ptychography, *Opt. Express* **26**, 3108 (2018).
- [31] M. Odstrčil, P. Baksh, S. A. Boden, R. Card, J. E. Chad, J. G. Frey, and W. S. Brocklesby, Ptychographic coherent diffractive imaging with orthogonal probe relaxation, *Opt. Express* **24**, 8360 (2016).